The American Journal of Human Genetics, Volume *104*

Supplemental Data

Bi-allelic Mutations in *TTC21A* Induce Asthenoteratospermia in Humans and Mice

Wangjie Liu, Xiaojin He, Shenmin Yang, Raoudha Zouari, Jiaxiong Wang, Huan Wu, Zine-Eddine Kherraf, Chunyu Liu, Charles Coutton, Rui Zhao, Dongdong Tang, Shuyan Tang, Mingrong Lv, Youyan Fang, Weiyu Li, Hong Li, Jianyuan Zhao, Xue Wang, Shimin Zhao, Jingjing Zhang, Christophe Arnoult, Li Jin, Zhiguo Zhang, Pierre F. Ray, Yunxia Cao, and Feng Zhang

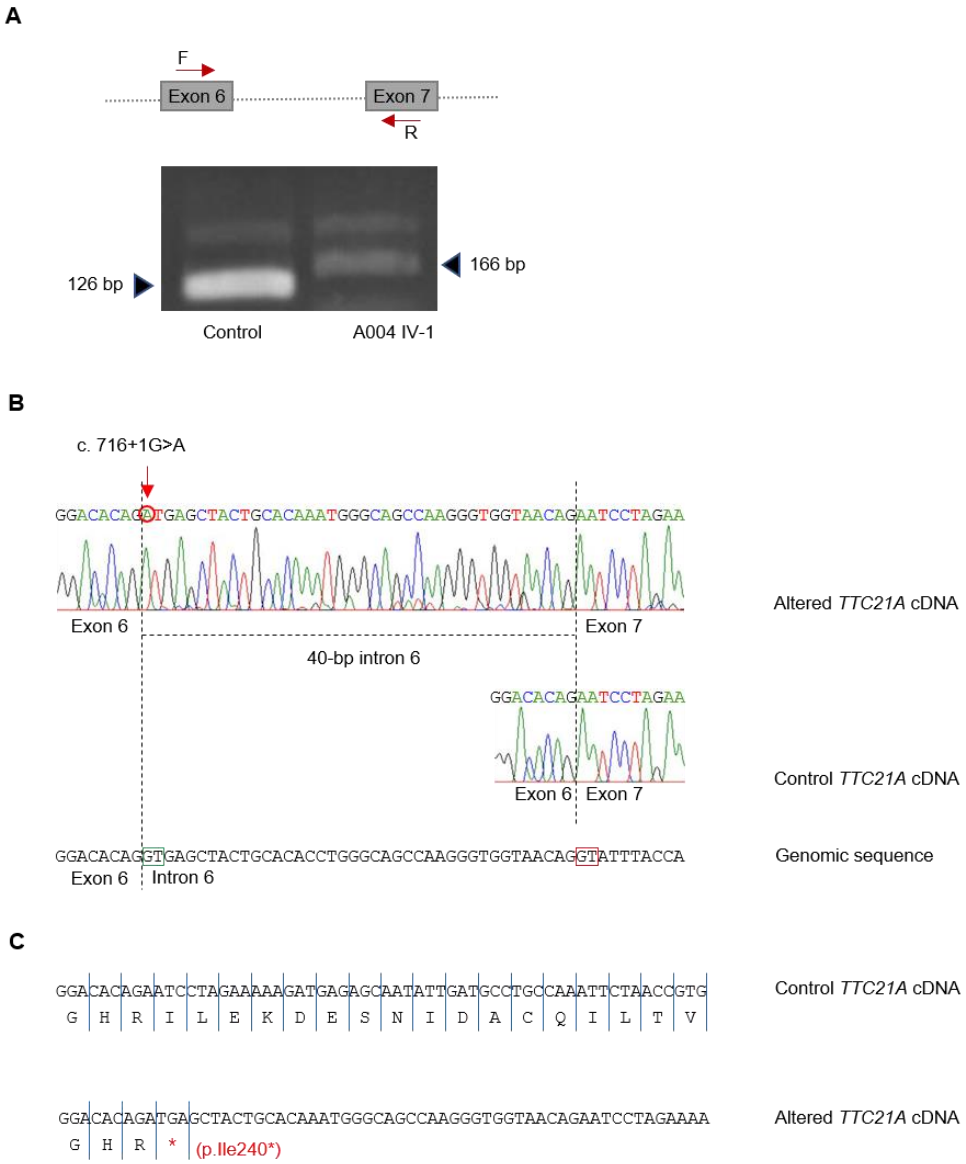

Figure S1. Splicing Alteration Caused by the *TTC21A* Splice-Site Mutation in Human Subject A004 IV-1.

(A) The forward and reverse primers were respectively designed in exons 6 and 7 of *TTC21A* for amplification and sequencing of cDNA. The RT-PCR product obtained from subject A004 IV-1 is longer than that from the control subject. (B) Sanger sequencing revealed a 1 bp substitution of c.716+1G>A (red arrow) at the splice donor site of intron 6. This splice-site mutation resulted in the partial retention of intron 6. The aberration can be explained by the utilization of a downstream cryptic splice donor site (red rectangle) in intron 6 instead of the normal splice donor site (green rectangle). (C) Immediate premature stop codon (p.Ile240*) was predicted according to the altered cDNA sequence of *TTC21A*.

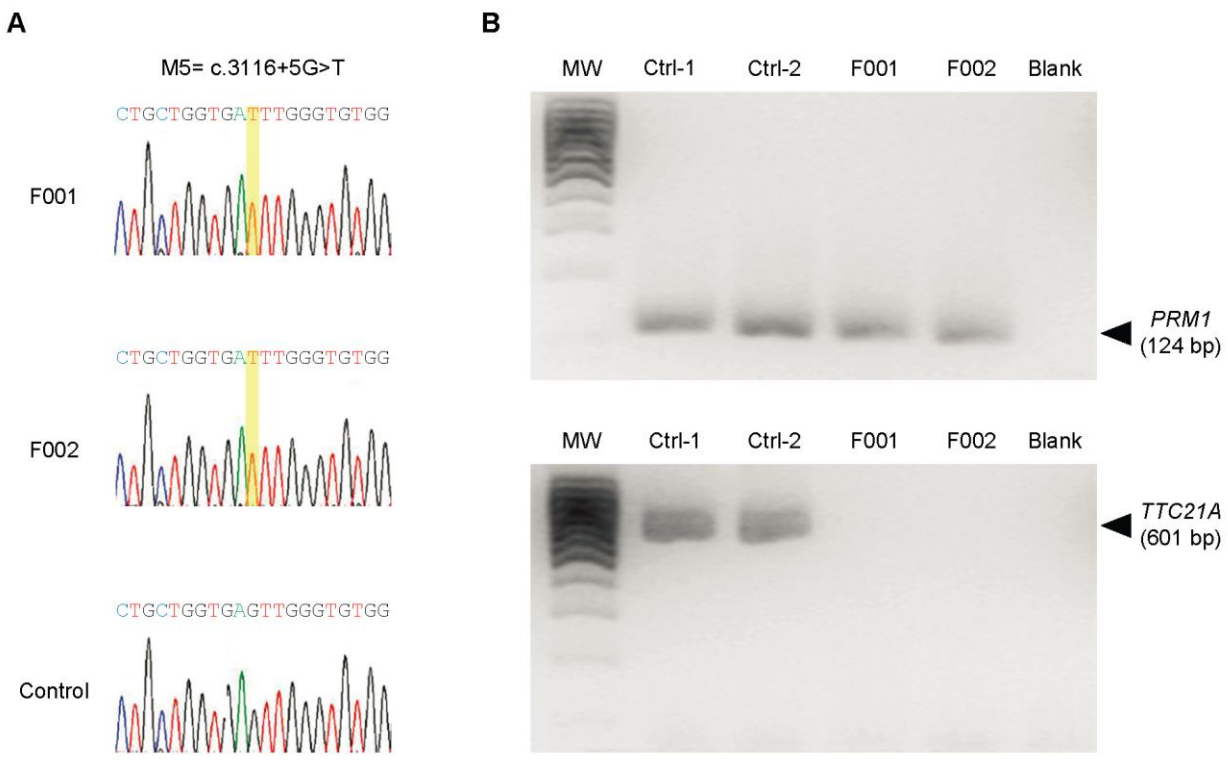

Figure S2. A Homozygous Splicing Mutation of *TTC21A* in Two Unrelated Tunisian Men with MMAF.

(A) The homozygous splicing mutation (c.3116+5G>T) of *TTC21A* was newly identified in two Tunisian men by WES and was further confirmed by Sanger sequencing. (B) To investigate potential deleterious effect of the splicing variant c.3116+5G>T, total RNA was extracted from sperm samples of these two *TTC21A*-mutated subjects (F001 and F002). The amplification of a cDNA sequence ranging from exons 21 to 26 yielded a normal band of 601 bp in control samples (Ctrl-1 and Ctrl-2) whereas no amplification was detected from sperm samples of two *TTC21A*-mutated subjects. *PRM1* was used as an internal control gene.

Figure S3. The Frameshift Mutation c.2534del Generated in the Mouse *Ttc21a*.
(A) A *Ttc21a* frameshift mutation c.2534del (*Ttc21a*^{mut}) was generated in mice using CRSIPR-Cas9 technology. The deleted nucleotide was shown by a red dash. (B) This frameshift mutation was predicted to cause premature translational termination (p.Lys845Argfs*5) of *Ttc21a*. The termination codon (red asterisk) was shown in the mutated cDNA.

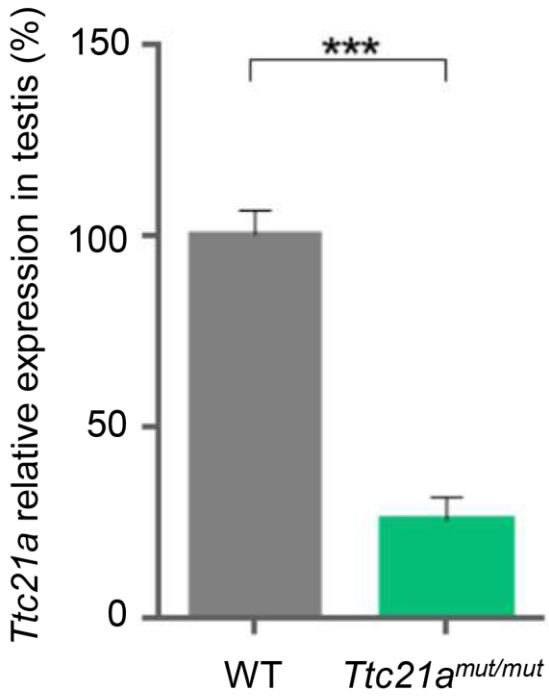

Figure S4. Expression Analysis of *Ttc21a* mRNA in the *Ttc21a*-Mutated Male Mice.
RT-qPCR assays showed that the mRNA level of *Ttc21a* in testes of the *Ttc21a*-mutated mice (*Ttc21a*$^{mut/mut}$) was reduced to approximately 26% of that in the wild-type (WT) mice. At least three testes were used for biological replicates. The internal control gene used for these assays was *Gapdh*. Each sample was assayed in triplicate for technical replicates. Error bars represent the standard error of the mean. *** $P < 0.001$ (Student's *t*-test).

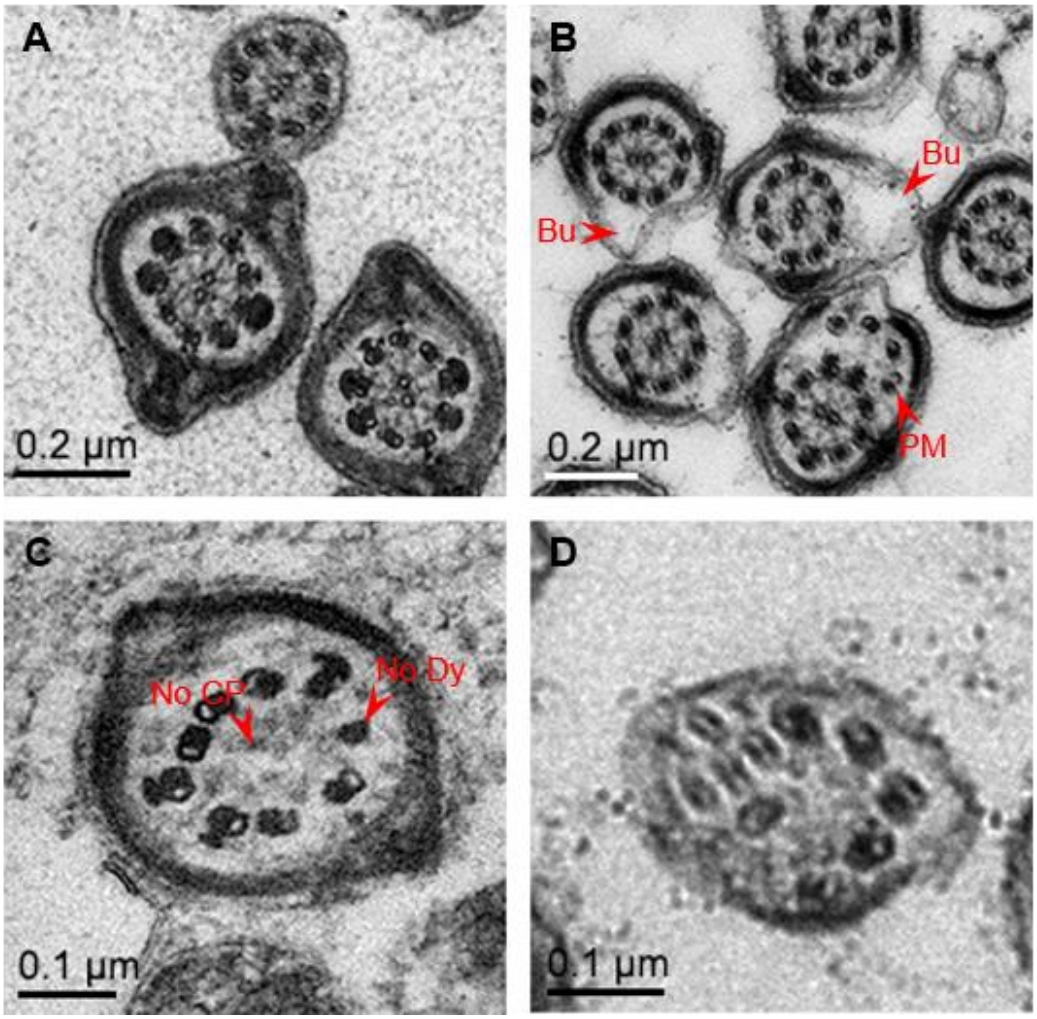

Figure S5. TEM Analyses of Spermatozoa from the *Ttc21a*-Mutated Male Mice Revealed Defects of the Flagella.

(A) The cross sections of normal spermatozoa from the WT male mice showed typical "9+2" microtubule structures. (B-D) Multiple structural abnormalities were observed in the sperm flagella of the *Ttc21a*-mutated male mice (*Ttc21a*$^{mut/mut}$). These structural abnormalities included abnormal bulges (Bu), extra peripheral microtubule doublets (PM), lacks of central-pair microtubules (CP), absent dynein arms (Dy), and abnormal arrangement of the nine peripheral microtubule doublets.

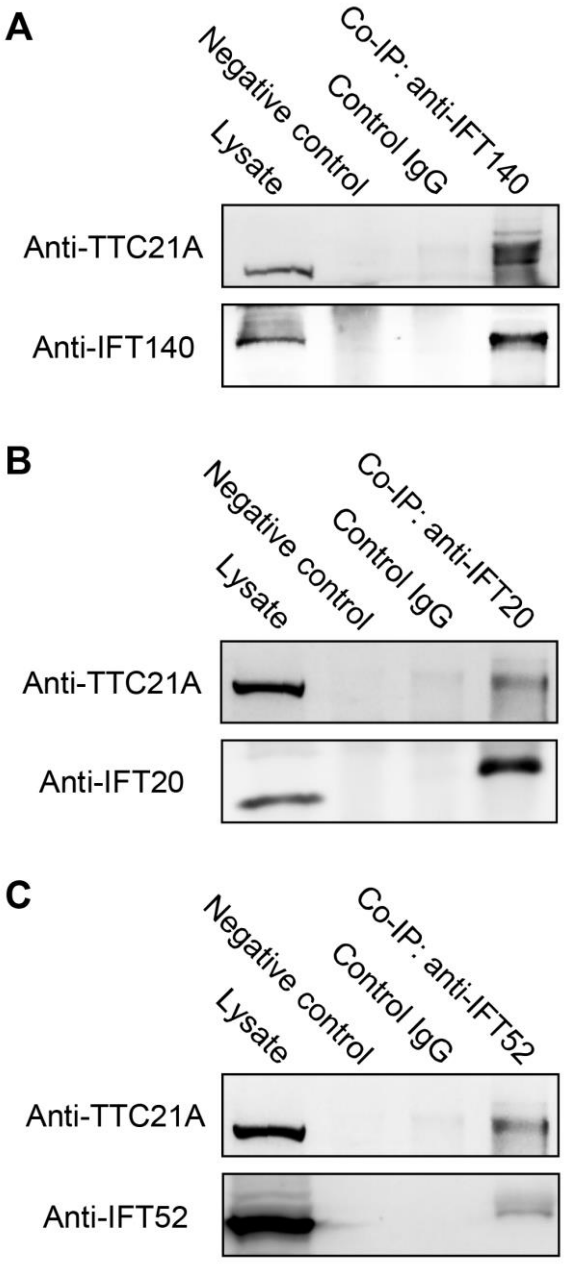

Figure S6. Co-Immunoprecipitation (Co-IP) Assays of Human Spermatozoa Revealed the Interactions between TTC21A and Known IFT Proteins.

Total protein was extracted from semen samples of human control subjects. Co-IP assays were respectively performed with the IFT antibodies (Proteintech, USA), including anti-IFT140 (A), anti-IFT20 (B) anti-IFT52 (C). Protein A agarose beads (EMD Millipore, USA) were used for enrichment. The negative control only contained protein A beads without any antibody. Lysate was also immunoprecipitated with normal rabbit IgG (Abcam, UK) as controls. Western blot experiments were performed using anti-TTC21A (Abcam, UK) and the corresponding IFT antibodies. The positive TTC21A signals were detected in lysate and Co-IP groups, suggesting the interactions between TTC21A and these known IFT proteins.

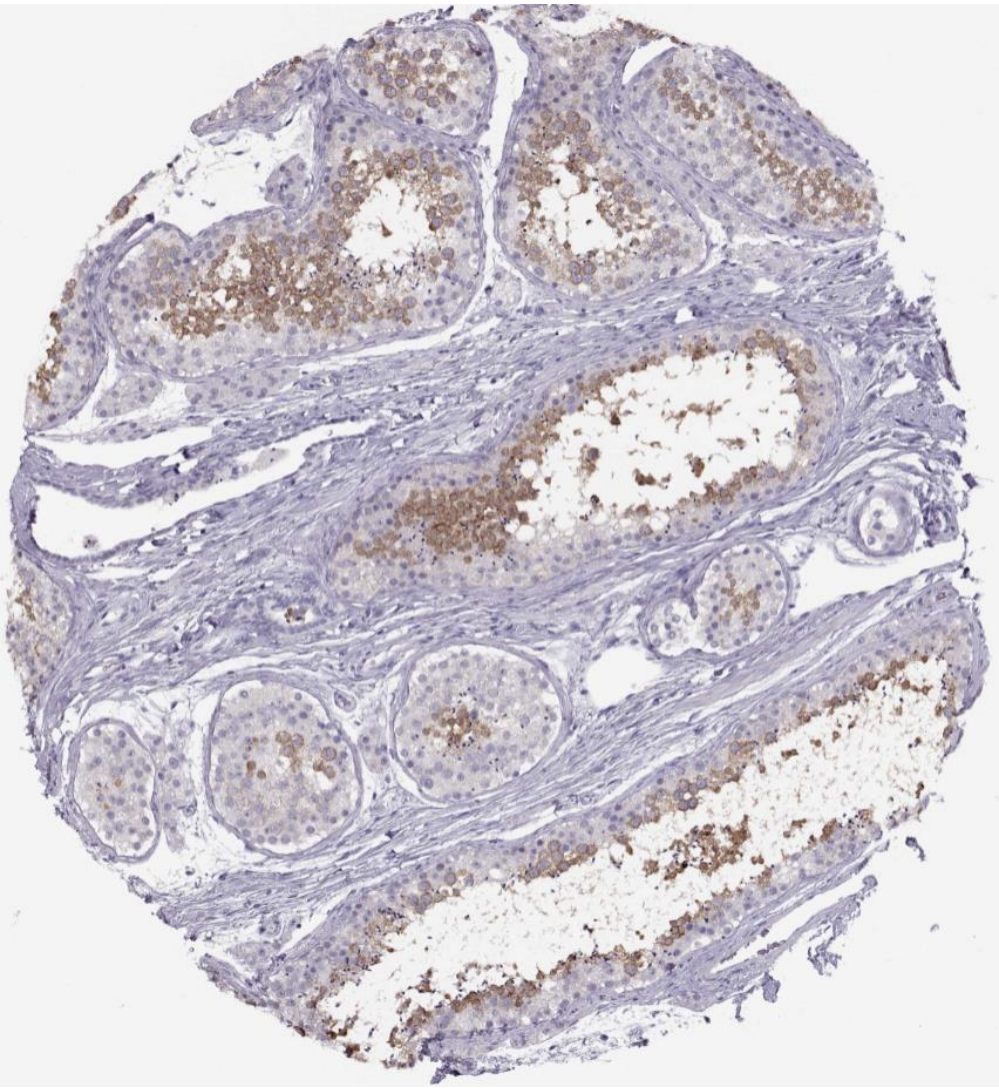

Figure S7. TTC21A is specifically expressed in the germ cell lineage.

The image of immunohistochemical staining in human testicular tissue is available from the Human Protein Atlas. Specific TTC21A staining is detected in preleptotene spermatocytes, pachytene spermatocytes, round spermatids, and elongated spermatids, suggesting that TTC21A may play an important role in spermatogenesis.

Web link: https://www.proteinatlas.org/ENSG00000168026-TTC21A/tissue/testis#img

Table S1. Primers Used for Amplification and Verification of the *TTC21A* Mutations

Primer Name	Primer Sequence (5'-3')	Tm
M1-F	CTTTTCACTTTAGGCTATGTTCTGGAGGGG	61 ℃
M1-R	GTGTACCATAACTGAATGAACCAGGACGGG	
M2-F	TGACCTCACATGGCCTTACCCTATC	61 ℃
M2-R	ATTCTAGTCTCATTCTCCTGCCAGT	
M3-F	TGGCCTAACTACAGAGATGGATGTG	60 ℃
M3-R	TCTTTAACTTCAGGAGCAGTTTGCC	
M4-F	GATCTTGTCAGAAAAACCAAGCCAA	60 ℃
M4-R	TGGTGCAAGCCATAGAAAATCTATC	

Table S2. Primers Used for Functional Investigations on the *TTC21A* Splice-Site Mutation c.716+1G>A

Primer Name	Primer Sequence (5'-3')	Tm
A004-cDNA-F	CTTTTCACTTTAGGCTATGTTCTGGAGGGG	61 ℃
A004-cDNA-R	GTGTACCATAACTGAATGAACCAGGACGGG	

Table S3. Primers Used for Functional Investigations on the *TTC21A* Splicing Mutation c.3116+5G>T

Primer Name	Primer Sequence (5'-3')	Product Size (bp)
PRM1-F1	TGACTCACAGCCCACAGAGT	124
PRM1-R1	CTGCGACAGCATCTGTACCT	
*TTC21A*_RT-F1	CGCTTCTGTGTTGATGGCTG	601
*TTC21A*_RT-R1	CTTCTCAGCCTGCGCTATCT	

Table S4. Primers Used for Mouse *Ttc21a* Genotyping

Primer Name	Primer Sequence (5'-3')	Tm
Ttc21a-F	ATTACTACGAGGCTGCCCAGAAGAT	61 ℃
Ttc21a-R	CAAAGGTGTAGACTGAGGGAGCAGA	

Table S5. Primers Used for RT-qPCR Analysis

Primer Name	Primer Sequence (5'-3')	Tm
Ttc21a-RT-F	GTGGGCCTAGAGAGGTACAG	60 ℃
Ttc21a-RT-R	GTGGGCCTAGAGAGGTACAG	
Gapdh-F	GTGGGCCTAGAGAGGTACAG	60 ℃
Gapdh-R	TGAAGGGGTCGTTGATGGC	

Table S6. Semen Characteristics, Sperm Morphology and Ultrastructural Abnormalities in the *Ttc21a*-Mutated Male Mice

	Wild-Type Male Mice [a]	*Ttc21a*$^{mut/mut}$ Male Mice [a]
Semen Parameters		
Semen count (10^6) [b]	6.5 (6.0-7.1)	6.4 (6.0-7.2)
Motility (%)	84 (78-90)	39 (0-86)
Progressive motility (%)	74 (62-87)	33 (0-79)
Sperm Morphology		
Normal spermatozoa (%)	83.3 (83.0-90.0)	26.7 (1.0-74.0)
Abnormal head-tail conjunction (%)	4.9 (3.0-10.0)	60.7 (16.5-92.5)
Short flagella (%)	1.0 (0.5-2)	10.5 (0.5-29.5)
Coiled flagella (%)	2.0 (1.5-2.0)	6.1 (2.0-14.5)
Angulation (%)	0 (0-0)	2.0 (0-4.5)
Irregular caliber (%)	0 (0-0)	0.3 (0-1.0)
Flagellar Ultrastructural Abnormalities [c]		
Abnormal principle pieces (%)	3.4 (2.4-5.2)	17.2 (5.0-27.3)
Abnormal end pieces (%)	2.3 (0.3-3.5)	32.6 (15.6-46.2)

[a] Values represent the mean (range).

[b] Per single epididymis.

[c] More than one hundred cross sections were analyzed.

Table S7. Distributions of the *TTC21A* Loss-of-Function (LoF) Alleles in Our Chinese MMAF Cohort and the Human Populations Archived by the ExAC Database

***TTC21A* Allele**	**Chinese MMAF**	**ExAC**	***P* Value ***
Allele numbers of LoF variants	5	148	7.01×10^{-7}
Allele numbers of non-LoF variants	125	122824	

* Two tailed Fisher's exact test

Supplemental Methods

Whole-Exome Sequencing and Bioinformatic Analysis

The DNeasy Blood and Tissue Kit (QIAGEN, Germany) was employed to extract genomic DNAs from peripheral blood samples of human subjects and their available parents. The whole human exome was enriched and constructed as a DNA library using the SureSelect^{XT} Human All Exon Kit (Agilent, USA). Next-generation sequencing was carried out on the HiSeq X-TEN platform (Illumina, USA). Sequencing reads were aligned to the human genome reference assembly (GRCh37/hg19) using the Burrows-Wheeler Aligner.[1] We employed the Picard software to remove PCR duplicates and evaluate the quality of variants. The Genome Analysis Toolkit was employed to call and analyze single-nucleotide variants (SNVs) and indels.[2] The SNVs with read depths less than 4× were filtered out. Then, functional information on genetic variants from the Gene Ontology Consortium, Sorting Intolerant From Tolerant (SIFT), Polymorphism Phenotyping v2 (PolyPhen-2), MutationTaster, the Exome Aggregation Consortium (ExAC) Browser and KEGG pathway databases were annotated through the ANNOVAR tool.[3-9] The Online Mendelian Inheritance in Man (OMIM) database was also used for functional annotation in this study.

Male infertility is potentially exposed to strong purifying selection because of the defects to natural conception. Therefore, the pathogenic variants responsible for MMAF cannot be common in the general populations. In this study, the genetic variants with allele frequencies ≥ 0.01 in the human population genome databases (e.g., the ExAC Browser and 1000 Genomes Project) were excluded.[9,10] Nonsense, frameshift and essential splice-site variants were preferred. Missense variants predicted to be deleterious by SIFT, PolyPhen-2, and/or MutationTaster were also included for further analyses. Previous studies have so far only demonstrated the autosomal recessive inheritance for human MMAF.[11] Therefore, homozygous or compound heterozygous variants were kept for further verification.

Semen Analysis

Semen samples of human subjects were collected by masturbation after 2-7 days of sexual abstinence, and were examined after liquefaction for 30 min at 37 ℃. Analyses of semen volume, sperm concentration, and motility were carried out and replicated in the source hospitals during routine biological examination according to the 5th World Health Organization (WHO) guidelines.

Sperm samples of mice were from the cauda epididymides, and were obtained by dissection of adult male mice followed by incubation in 1 mL solution of capacitation for 15 min at 37 ℃. Semen characteristics were evaluated using the computer-assisted sperm analysis (CASA) system.

Transmission Electron Microscopy

Semen samples were washed and fixed routinely, and then were progressively dehydrated with graded ethanol (50%, 70%, 90%, and 100%) and 100% acetone. After drying and embedding, the specimens were sliced with ultra-microtome and stained with uranyl acetate and lead citrate. The slices were observed and photographed by TEM (TECNAI-10, Philips) with an accelerating voltage of 80 kV.

Supplemental References

1. Li, H., and Durbin, R. (2010). Fast and accurate long-read alignment with Burrows-Wheeler transform. Bioinformatics *26*, 589-595.
2. McKenna, A., Hanna, M., Banks, E., Sivachenko, A., Cibulskis, K., Kernytsky, A., Garimella, K., Altshuler, D., Gabriel, S., Daly, M., et al. (2010). The Genome Analysis Toolkit: a MapReduce framework for analyzing next-generation DNA sequencing data. Genome Res. *20*, 1297-1303.
3. Wang, K., Li, M., and Hakonarson, H. (2010). ANNOVAR: functional annotation of genetic variants from high-throughput sequencing data. Nucleic Acids Res. *38*, e164.
4. Ashburner, M., Ball, C.A., Blake, J.A., Botstein, D., Butler, H., Cherry, J.M., Davis, A.P., Dolinski, K., Dwight, S.S., Eppig, J.T., et al. (2000). Gene ontology: tool for the unification of biology. The Gene Ontology Consortium. Nat. Genet. *25*, 25-29.
5. Kanehisa, M., Furumichi, M., Tanabe, M., Sato, Y., and Morishima, K. (2017). KEGG: new perspectives on genomes, pathways, diseases and drugs. Nucleic Acids Res. *45*, D353-D361.
6. Kumar, P., Henikoff, S., and Ng, P.C. (2009). Predicting the effects of coding non-synonymous variants on protein function using the SIFT algorithm. Nat. Protoc. *4*, 1073-1081.
7. Adzhubei, I.A., Schmidt, S., Peshkin, L., Ramensky, V.E., Gerasimova, A., Bork, P., Kondrashov, A.S., and Sunyaev, S.R. (2010). A method and server for predicting damaging missense mutations. Nat. Methods *7*, 248-249.
8. Schwarz, J.M., Cooper, D.N., Schuelke, M., and Seelow, D. (2014). MutationTaster2: mutation prediction for the deep-sequencing age. Nat. Methods *11*, 361-362.
9. Lek, M., Karczewski, K.J., Minikel, E.V., Samocha, K.E., Banks, E., Fennell, T., O'Donnell-Luria, A.H., Ware, J.S., Hill, A.J., Cummings, B.B., et al. (2016). Analysis of protein-coding genetic variation in 60,706 humans. Nature *536*, 285-291.
10. 1000 Genomes Project Consortium, Abecasis, G.R., Auton, A., Brooks, L.D.,

DePristo, M.A., Durbin, R.M., Handsaker, R.E., Kang, H.M., Marth, G.T., and McVean, G.A. (2012). An integrated map of genetic variation from 1,092 human genomes. Nature *491*, 56-65.

11. Ben Khelifa, M., Coutton, C., Zouari, R., Karaouzene, T., Rendu, J., Bidart, M., Yassine, S., Pierre, V., Delaroche, J., Hennebicq, S., et al. (2014). Mutations in DNAH1, which encodes an inner arm heavy chain dynein, lead to male infertility from multiple morphological abnormalities of the sperm flagella. Am. J. Hum. Genet. *94*, 95-104.